Analyst

PAPER

View Article Online
View Journal

Cite this: DOI: 10.1039/c8an02261e

Sensors for biosensors: a novel tandem monitoring in a droplet towards efficient screening of robust design and optimal operating conditions†

Daria Semenova, *[a] Yuliya E. Silina, [b] Marcus Koch,[b] Laura Micheli, [c] Alexandr Zubov [a] and Krist V. Gernaey [a]

Understanding the biorecognition and transduction mechanisms is a key aspect in the development of robust sensing technologies. Therefore, the design of tools and analytical approaches that could allow gaining a deeper insight into the bio- and electrochemical processes would significantly accelerate the progress in the field of biosensors. Herein, we present a novel effective strategy for biosensor design screening based on tandem monitoring of individual system parameters in a droplet. The developed tandem approach couples the simultaneous chronoamperometric characterization of biosensors in the presence of an analyte (glucose) together with dissolved oxygen monitoring using a luminescence-based optical oxygen microsensor. Remarkably, an optical sensor was applied for the first time to analyse the amperometric biosensor response and kinetics. Two types of multi-layer glucose biosensors (first generation) were chosen as a case study and were evaluated at various operating conditions using multi-analytical techniques. Moreover, specific protocols were developed for the detection of oxygen conversion rates, iron and membrane elution inside the multi-layer glucose biosensor system. The presented tandem monitoring approach allows one to identify and build-up the correlations between the critical operation conditions and system parameters affecting the overall biosensor response, its sensitivity and lifetime. Thus, based on the obtained experimental results a more favorable composition of Nafion membrane films and enzyme loadings for glucose biosensors were identified in a time-efficient way and allowed to explain an improved stability (up to 3 months) and linear detection range of glucose concentrations (up to 5 mM). Furthermore, the presented tandem monitoring approach can be readily adapted to other oxygen dependent types of biosensors either for simultaneous multiple substrate detection or as an efficient tool for biosensor design and operating condition screening.

Received 21st November 2018,
Accepted 3rd February 2019

DOI: 10.1039/c8an02261e

rsc.li/analyst

1. Introduction

More than 50 years of glucose biosensor research have been mainly focused on the evolution of biosensors[1–4] towards the accurate and non-invasive application in diabetes management and treatment.[5,6] Unfortunately, almost no attempts were done towards the development of unexpansive analytical approaches or screening platforms with quick read-out capabilities allowing time-efficient screening of biosensor design and operating conditions. As a result, the promotion of robust sensing technologies for continuous glucose monitoring still remains a challenge either in clinical diagnostics[7,8] or for fermentation processes.[9–11] The required selectivity and sensitivity of the biosensors towards the analyte of interest can be fine-tuned by combining specific bioreceptors (*e.g.* enzymes, whole cells, biomimetic receptors, *etc.*) together with various configurations (*i.e.* surface arrangement and architecture) of electrode materials (*e.g.* carbon-based materials, noble metals, *etc.*).[12–16] However, the presence of low and high molecular weight substances in biological samples would interfere with the desired analyte sensing and affect the overall electrochemical behaviour of the system. Moreover, the accumulation of such active compounds on the electrode surface would lead to irreversible changes in biosensor topology including bioreceptor deactivation, membrane pore blockage, reference electrode oxidation, mediator and/or membrane layer leakage, finally resulting in a decrease of the biosensor response.

[a]*Process and Systems Engineering Center (PROSYS), Department of Chemical and Biochemical Engineering, Technical University of Denmark, Søltofts Plads, Building 229, 2800 Kgs. Lyngby, Denmark. E-mail: dsem@kt.dtu.dk*
[b]*INM – Leibniz Institute for New Materials, Campus D2 2, 66123 Saarbrücken, Germany*
[c]*Department of Chemical Science and Technologies, Università di Roma Tor Vergata, Via della Ricerca Scientifica 1, 00133 Rome, Italy*
†Electronic supplementary information (ESI) available. See DOI: 10.1039/c8an02261e

Since the biosensor lifetime depends not only on the storage stability factors (*e.g.* dry or wet storage, temperature, *etc.*) but is mainly defined by the aspect of operational stability (*e.g.* sensor design, experimental and operational conditions, *etc.*),[17–19] various strategies were applied to improve the overall biosensor characteristics. Therefore, in the past few years a great variety of biocompatible membranes and coating materials have been developed to partly eliminate the above-mentioned interactions and to improve the overall biosensor performance.[20] The application of anti-interference membranes decreases the impact of thickness fluctuations and during the exploitation of biosensors with biological samples increases the concentration gradients inside the system which minimizes the risk of bioreceptor layer inactivation on the one hand, and can also lead to an increased response time and affect the sensitivity on the other hand. One of the most widely used polymers for enzyme encapsulation is the perfluorinated membrane Nafion®. Initially supplied as a proton exchange membrane for fuel cells by DuPont,[21,22] this sulfonated tetrafluorethylene-based copolymer played an important role in the development of glucose biosensors.[23–26] Moreover, the influence of the number of membrane films and their composition on the response[27] and long-term lifetime[28,29] was demonstrated experimentally for implantable glucose biosensors. Since Nafion structure units are not covalently cross-linked, it allows transforming them into a variety of shapes. However, the morphology of the Nafion ionomer thin films used in biosensors and their behaviour under various operating conditions are fundamentally different from membranes and is still not very well understood.[30] Therefore, different analytical and simulation approaches, including the effect of temperature,[26] alcohol/water solutions[31,32] and presence/absence of glucose during chronopotentiometric characterization,[33] were applied to investigate the structure and transport phenomena of wetted Nafion films.[34,35] Moreover, it was demonstrated that combining Nafion® membranes with novel transducer materials with enhanced electron transport (*e.g.* exfoliated graphite nanoplatelets) can significantly improve the stability, sensitivity and linear detection range of biosensors.[36] However, the lack of more in-depth knowledge and understanding about the correlation between the membrane film properties and biosensor operational stability in the presence of a substrate (*i.e.* glucose) are the two major impediments towards the design of truly robust biosensors. Ivanauskas *et al.*[37] with the help of mathematical models compared the theoretical response of two types of biosensors containing a single heterogeneous enzyme layer and an additional protecting membrane (polymer-based) layer. From the obtained simulation results it was concluded that by varying the activity of the enzyme together with the design, thickness and properties of the membrane, the biosensor performance can be significantly improved. However, the biosensor stability measurements are time and resource consuming which could easily explain why no experimental validation was presented.

Therefore, the main objective of the presented work was in the development of a tandem monitoring approach that allows the simultaneous on-line detection of multiple biosensor system parameters. Although the combination of electrochemical and optical methods has already been applied for the independent detection of a desired analyte,[38] a tandem monitoring approach based on using luminescence-based optical sensors to analyse the amperometric biosensor response and kinetics has not been previously reported. Since only well investigated materials and systems can be applied at the initial development and validation stages of the novel screening platforms, glucose biosensors with confirmed stability (based on a premixed enzyme and a 2 vol% Nafion®117 membrane layer referred to as *sensor 3* batch) were used as a case study following our previous work.[39] Moreover, their performance was compared with a new sensor architecture containing individual enzyme and outer membrane (2 vol% Nafion®117) coatings. The factors underlying variation in a lifetime and performance of the glucose biosensors, namely sensitivity, linear calibration range and detection limits, were identified and analysed in the presence of a substrate (glucose). The electrochemical behaviour (cyclic voltammetry and chronoamperometry) of both types of biosensors was fully characterized using multi-analytical techniques, including morphological investigation of the layer-by-layer deposition by scanning electron microscopy (SEM) coupled with energy dispersive X-ray spectroscopy (EDX) and quantification of mediator and Nafion®117-based layer stability by means of inductively coupled plasma mass spectrometry (ICP-MS) and liquid chromatography-electrospray ionization-tandem mass spectrometry (LC-ESI-MS/MS), respectively. Moreover, the swelling behaviour of the membrane films under dynamic conditions and the impact of environmental conditions, *viz.* temperature and humidity, on their stability during formation were investigated by using the environmental detection module of a scanning electron microscope (ESEM).

2. Experimental section

2.1. Reagents and materials

The DRP-PW-110DGPHOX screen printed electrodes (SPEs) were customized by DropSens (Llanera, Spain) and ItalSens IS-C was acquired from PalmSens (Utrecht, The Netherlands). Both types of electrodes were printed on a polyester substrate and each sensor consists of a carbon working electrode (modified with a graphene oxide layer for DRP-PW-110DGPHOX), a carbon counter electrode and a silver reference electrode. The diameter of the working electrodes was 0.4 cm (DRP-PW-110DGPHOX) and 0.3 cm (ItalSens IS-C), resulting in apparent geometric areas of 0.126 cm^2 and 0.07 cm^2, respectively.

Glucose oxidase (GOx) (EC 1.1.3.4, type VII, 248 U g^{-1} solid) and bovine serum albumin (BSA) were obtained from Sigma (St Louis, MO, USA). Glutaraldehyde solution (25% (v/v)), ethanol (UV HPLC gradient, 99.9%) and potassium hexacyanoferrate(III) (ACS reagent, ≥99.0%) were purchased from Sigma –

Aldrich (St Louis, MO, USA). Iron(III) chloride (anhydrous, 99.99%) and Nafion®117 solution (~5% (v/v) in a mixture of lower aliphatic alcohols and water) were provided by Aldrich (Steinheim, Germany). D-Glucose (anhydrous) was provided by Fluka (Loughborough, UK). Mono – and di-potassium hydrogen phosphates (anhydrous) were obtained from Merck (Darmstadt, Germany). Sodium hydroxide (50% (w/w)) and hydrochloric acid (37% (w/w)) solutions were purchased from VWR International A/S (Søborg, Denmark). All the solutions were prepared with 0.1 M phosphate buffer supplemented with 0.1 M KCl (pH = 6), unless stated otherwise.

2.2. Glucose biosensor preparation

To avoid biosensor surface modification prior to the modification steps no pre-treatment in phosphate buffer solution under chronoamperometric conditions was applied. The optimized preparation methods for Prussian Blue deposition and the membrane composition were acquired for *sensor 3* batch from Semenova *et al.*[39] Therefore, after the glutaraldehyde layer over the PB modified working electrode was dried, the premixed enzyme/membrane or individual enzyme and membrane layers were deposited. To simplify the reference to the specific glucose biosensor preparation method, the "two" and "four" layer sensor terminology (see Fig. S1 ESI†) will be introduced below. The "two" layer glucose biosensors represent the *sensor 3* batch from ref. 39. A 3 μL drop of Nafion®117 (2 vol%) neutralized in ethanol[40] mixed with GOx dissolved in phosphate buffer and BSA (5 vol% diluted in water) in a 1 : 1 : 1 proportion (v/v/v) was placed over PB/glutaraldehyde modified SPEs. For the "four" layer glucose biosensors the glutaraldehyde solution layer was dried and then a 3 μL drop of GOx dissolved in phosphate buffer mixed with BSA (5 vol% diluted in water) in a 1 : 1 proportion (v/v) was placed over the surface of the WE. The Nafion®117 (2 vol% neutralized in ethanol) membrane layer (3 μL) was deposited over the SPE/PB/Glut/(GOx + BSA) modified electrodes no less than 20 hours from the previous layer immobilization step. An additional layer (3 μL) of fresh Nafion®117 (2 vol% neutralized in ethanol) solution was deposited after 24–32 hours. Regardless of the biosensor design, the SPEs with the deposited enzyme and/or membrane layers were placed to dry overnight in a climate chamber at 40% of humidity and 8 °C. Moreover, both PB modified SPEs and complete glucose biosensors were stored in the dark, at room temperature and 4 °C, respectively.

2.3. Glucose oxidase stock activity measurements

Similar to the previously described procedure in ref. 39, the activity of the GOx stock solutions, as well as the enzyme/membrane or enzyme/BSA mixtures, was estimated prior to the immobilization step using an OXSOLV solvent-resistant, fiber – optic oxygen sensor (PyroScience GmbH, Aachen, Germany) connected to a FireStingO2 fiber – optic meter (PyroScience GmbH, Aachen, Germany) and controlled by Pyro Oxygen Logger software (PyroScience GmbH, Aachen, Germany). The measurement was performer *via* on-line monitoring of the consumption rates for the dissolved oxygen (DO) in the reaction of 100 mM glucose solution with two types of GOx stock solutions (A and B) at room temperature. The setup assembly, as well as the experimental procedure, were previously described in ref. 39. For the enzyme activity calculations, one unit (U) of the enzyme corresponds to a substrate consumption of 1 μmol per min. The GOx activity prior to immobilization was estimated for Stock A as 0.548 U μL^{-1} and for Stock B equal to 0.871 U μL^{-1}. The glucose biosensors prepared for electrochemical and morphological analyses are summarized in Table S1 (see the ESI†).

2.4. Cyclic voltammetry characterization of glucose biosensors

Cyclic voltammetry (CV) characterization of the biosensor was carried out by using MultiEmStat (PalmSens, Utrecht, The Netherlands) with a DRP-CAST1X8 interface (DropSens, Llanera, Spain) controlled by MultiTrace 3.4 software (PalmSens, Utrecht, The Netherlands). In all experiments a 100 μL droplet of phosphate buffer was placed over all three electrodes of the SPE and the response was analysed in a potential range from −0.5 V to +0.5 V. A previously not tested biosensor was used each time a new scan rate was applied and the buffer probes collected after the measurements were further analysed by liquid chromatography tandem mass spectrometry (LC-MS/MS) and inductively coupled plasma mass spectrometry (ICP-MS). The voltammograms obtained for unmodified SPEs, PB modified electrodes, "two" and "four" layer glucose biosensors at 50 mV s^{-1} are compared in Fig. S1 (see the ESI†). The voltammograms recorded for both types of glucose biosensors at different scan rates (10, 20 and 50 mV s^{-1}) are summarized in Fig. S2 (see the ESI†). To compare the diffusion properties of both types of glucose biosensors, the dynamic response of the flavin adenine dinucleotide groups of immobilized glucose oxidase was studied in the presence of potassium ferricyanide. Similar to oxygen (see Fig. 1B), ferricyanide being an electron acceptor participates in a two-step reduction of the GOx flavin groups.[41] A 100 μL droplet of 0.01 M potassium ferricyanide prepared with phosphate buffer (pH = 7.4) was placed over all three electrodes of the "two" and "four" layer glucose biosensors. The CVs were registered for the same biosensor at different scan rates, namely 10, 20, 50 70 and 100 mV s^{-1} (see Fig. S2, ESI†).

2.5. Chronoamperometric characterization of glucose biosensors

Chronoamperometric (AM) studies were performed using MultiEmStat (PalmSens, Utrecht, The Netherlands) with a DRP-CAST1X8 interface (DropSens, Llanera, Spain) controlled by MultiTrace 3.4 software (PalmSens, Utrecht, The Netherlands). The biosensors were characterized in the presence of an analytical range of glucose concentrations (0 to 5 mM) at the applied voltage equal to the peak potential of the H_2O_2-reduction by Prussian Blue (−0.14 V). All measurements from the same biosensor type were repeated at least in triplicate. After the AM signal was registered, the buffer probes with

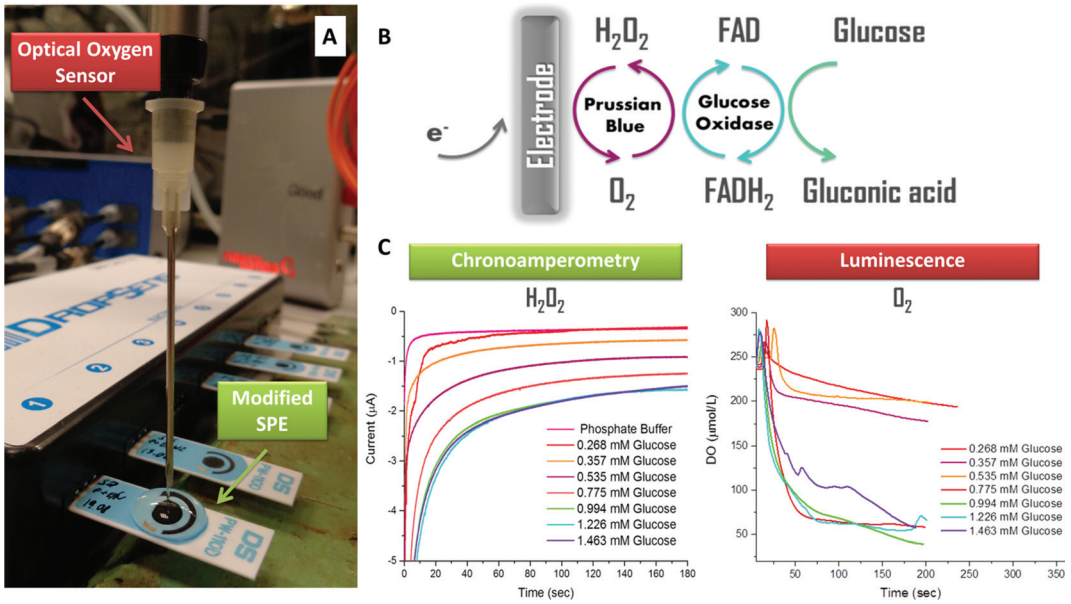

Fig. 1 The experimental setup (A) for the tandem oxygen and glucose monitoring in a droplet for free enzyme solutions and the enzyme immobilized on the surface of a modified screen-printed electrode (SPE). The schematic representation of the glucose biosensor operation principles is summarized in B. The glucose oxidase cofactor groups (FAD)/(FADH2) – oxidized/reduced forms are highlighted. The results of the chronoamperometric response towards the peroxide reduction by Prussian Blue and luminescence detection of the dissolved oxygen (DO) consumption rates by glucose oxidase in the presence of glucose are shown in C.

and without glucose were collected for subsequent LC-ESI-MS/MS and ICP-MS investigation.

2.6. Tandem oxygen and glucose monitoring

In order to simultaneously obtain the glucose and dissolved oxygen concentration profiles in a droplet, the chronoamperometry- and luminescence-based measurement tandem was applied. The PB modified SPEs or complete glucose biosensors were connected through an interface (DRP-CAST1X8) to the potentiostat (MultiEmStat) and the tip of the OXR430 retractable needle-type fiber-optic oxygen minisensor (PyroScience GmbH, Aachen, Germany) was centred close to the surface of the working electrode, as shown in Fig. 1A. The chronoamperometric and luminescence studies were based on the detection of hydrogen peroxide production and dissolved oxygen (DO) consumption during the glucose oxidase/glucose conversion, respectively (Fig. 1C). In order to compare the activity of the enzyme (GOx) immobilized on the biosensor surface towards the free enzyme solution two types of experiments were conducted. First, the activity of the freshly made free enzyme solution mixture of Stock B (GOx : BSA = 1 : 1 (v/v)) was estimated *via* tandem monitoring over the PB modified SPEs. A 200 μL (DropSens SPEs) or 300 μL (ItalSens SPEs) droplet of glucose solution of known concentration was placed over all three electrodes and the tip of the fiber optic minisensor was immersed inside the droplet close to the surface of the PB modified SPE and centred towards the working electrode. After the DO signal stabilized, simultaneously a 3 μL droplet of the enzyme mixture was added inside the glucose droplet and the −0.14 V potential was applied to the surface of the WE. The obtained results are summarized in Table S2 and Fig. S3 (see the ESI†).

The complete glucose biosensors (DropSens SPEs) with different layer compositions and immobilized enzyme stock solutions were analysed *via* tandem monitoring in the presence of glucose. The tip of the minisensor was centred towards the WE, and once a stable sensor response was obtained, simultaneously a 200 μL droplet of glucose solution of known concentration was placed over all three electrodes and the potential of −0.14 V was applied. The obtained results are summarized in Table S3 and Fig. S4 (see the ESI†). Regardless the type of the tandem monitoring applied (free or immobilized enzyme), the measurements were performed at room temperature for 180 s after the addition of enzyme mixtures or glucose solutions.

2.7. Scanning electron microscopy (SEM), energy dispersive X-ray spectroscopy (EDX) and environmental scanning electron microscopy (ESEM)

Micrographs of unmodified SPEs, "two" and "four" layer glucose biosensors after each layer modification were collected by scanning electron microscopy (SEM) using a FEI (Hilsboro, OR, USA) Quanta 400 FEG. Energy dispersive X-ray (EDX) analysis was done using an EDAX (Mahwah, NJ, USA) Genesis V 6.04 X-ray spectrometer in order to obtain knowledge about the chemical composition of the biosensor surfaces. The SEM/EDX protocols reported in our previous study[39] were applied. By correlative SEM/EDX analysis it was possible to determine the composition and morphology of the multi-layer biosensor for each deposition step (see Fig. S5, ESI†). To perform the membrane swelling experiments, the water saturated glucose

biosensors were analyzed using environmental scanning electron microscopy (ESEM) by varying the water vapor pressure inside the SEM chamber at a constant temperature (3 °C).

2.8. Liquid chromatography-electrospray ionization-tandem mass spectrometry (LC-ESI-MS/MS)

To verify and compare the chemical stability of the Nafion® membrane film for "two" and "four" layer glucose biosensors, liquid chromatography electrospray ionization tandem mass spectrometry (LC-ESI-MS/MS) was utilized. The protocol reported in our previous study[39] was applied. The MS/MS experiments were conducted in the product ion scan mode at collision energies ranging from 10 to 50 eV. The elemental compositions of the polymer membrane were identified based on accurate mass measurements and data processing of total ion chromatograms (TICs) and extracted ion chromatograms (EICs) of the parent ions and fragments obtained in the MS/MS experiments. From the obtained total ion chromatograms (TICs), characteristic perfluorinated carboxylic acid fragments,[42] namely $CF_3(CF_2)_5CHFCOO^-$ and $CF_3(CF_2)_6CHFCOO^-$, were detected and monitored in the EIC mode at m/z 394.9758 and 444.9725, respectively.

2.9. Inductively coupled plasma mass spectrometry (ICP-MS)

The samples collected after each scan during CV and AM measurements with regard to mediator layer stability (estimated as an amount of the Fe^{56} isotope migrated through the polymer membrane into the solution) were analyzed on a high resolution inductively coupled plasma mass spectrometer ELEMENT XR (Thermo Fisher Scientific, Bremen, Germany), equipped with an auto sampler SC-E2 DX (Elemental Scientific, Omaha, USA). To perform the experiments, a 10 μl buffer probe was diluted in 50 mL of 2% HNO_3 (pH = 2) and measured on the general Fe^{56} isotope content at medium resolution (MR), with the following source parameters: cool gas, 16.00 L min^{-1}; sample gas, 1.161 L min^{-1}; Faraday deflection, −217 V; plasma power, 1250 W; peristaltic pump speed, 10 rpm; torch X-Pos., 1.9 mm; torch Y-Pos., 0.8 mm; torch Z-Pos., −5.0 mm. High-purity argon (99.999%), a glass spray chamber, quartz-injector, Pt-sample and Ni-skimmer cones were used throughout the study. All calibration solutions, blank and samples were supplemented with 2% HNO_3 to set pH = 2 prior to ICP-MS analysis. The accuracy of ICP-MS quantification was verified by calculating the recoveries between the determined and expected concentration values.

3. Results and discussion

3.1. Glucose and oxygen tandem monitoring

Similar to the results previously presented in ref. 39, no significant difference in the voltammetric response was obtained between "two" and "four" layer biosensors, although distinct changes were made in the layer-by-layer assembly and membrane compositions. Thus, an equal linear increase in the current response following the increase in the scan rate was obtained for both types of glucose biosensors. Furthermore, the analogue diffusion properties of the membranes were demonstrated by scanning "two" and "four" layer glucose biosensors in the presence of potassium ferricyanide. To identify the difference in the biorecognition mechanism between the two types of biosensors, the simultaneous oxygen and glucose monitoring in a droplet was proposed.

In Fig. 2 the chronoamperometric response was demonstrated within the linear detection range for both "two" and "four" layer glucose biosensors (from 0.27 to 2 mM). Moreover, the sensitivity and detection limits were compared for "four" layer glucose biosensors having different activities of the immobilized glucose oxidase (Stock A, Stock B). From Fig. 2A it is clear that the sensitivity (slope value) and detection limits (glucose concentration range) significantly varied between the sensors. Note that the *4*layer Stock A* glucose biosensor has been previously characterized and the results presented in the graph correspond to the second calibration made three months later. Although, the "two" layer glucose biosensors showed a higher sensitivity (−1.6 μA mM^{-1} ± 0.13) with respect to both "four" layer sensors based on the GOx Stock A (−0.451 μA mM^{-1} ± 0.01) and Stock B (−0.915 μA mM^{-1} ± 0.05) solutions, the glucose detection limit is below a 1.23 mM concentration. Moreover, in Fig. 2B "four" layer glucose biosensors have demonstrated a lower standard deviation (between 0.02–0.2 μA mM^{-1}) and the sensors with immobilized GOx from Stock A were able to work with a broader range of glucose concentrations, as will be shown later in this section (see Fig. 3C). The analysis of the oxygen consumption rates obtained within tandem monitoring allowed explaining such variations in the biosensor response.

The microsensor was first applied for the real time measurement of oxygen conversion rates in the liquid phase (droplets) containing different glucose concentrations during the reaction with GOx from Stock A and Stock B immobilized on the surface of the above-mentioned biosensors. From Fig. 2C we can easily see that for Stock B based biosensors the increase of the oxygen consumption follows the increase in glucose concentration, however the oxygen deficit observed at 1.23 mM (see Table S3, ESI†) explains the limited detection range for "two" layer glucose biosensors. Therefore, the presence of the additional membrane films in the "four" layer biosensors prevents GOx from the direct contact with a higher glucose content and, although the level of the dissolved oxygen concentration for Stock B based enzymes is already low inside the droplet at 0.78 mM (see Table S3, ESI†), these biosensors are capable of working in a broader range of concentrations. Moreover, the obtained results are in good agreement with the earlier discussed theoretical studies of Ivanauskas *et al.*[37] Thereby, it was interesting to compare the behaviour of "four" layer biosensors with immobilized GOx that showed a different activity in the free enzyme stock solutions (for more details see Fig. 3). The biosensors based on Stock A solution, where the free enzyme showed almost 63% less activity compared to Stock B, maintained both the dissolved oxygen and the conversion rate in the droplet constant (see Table S3,

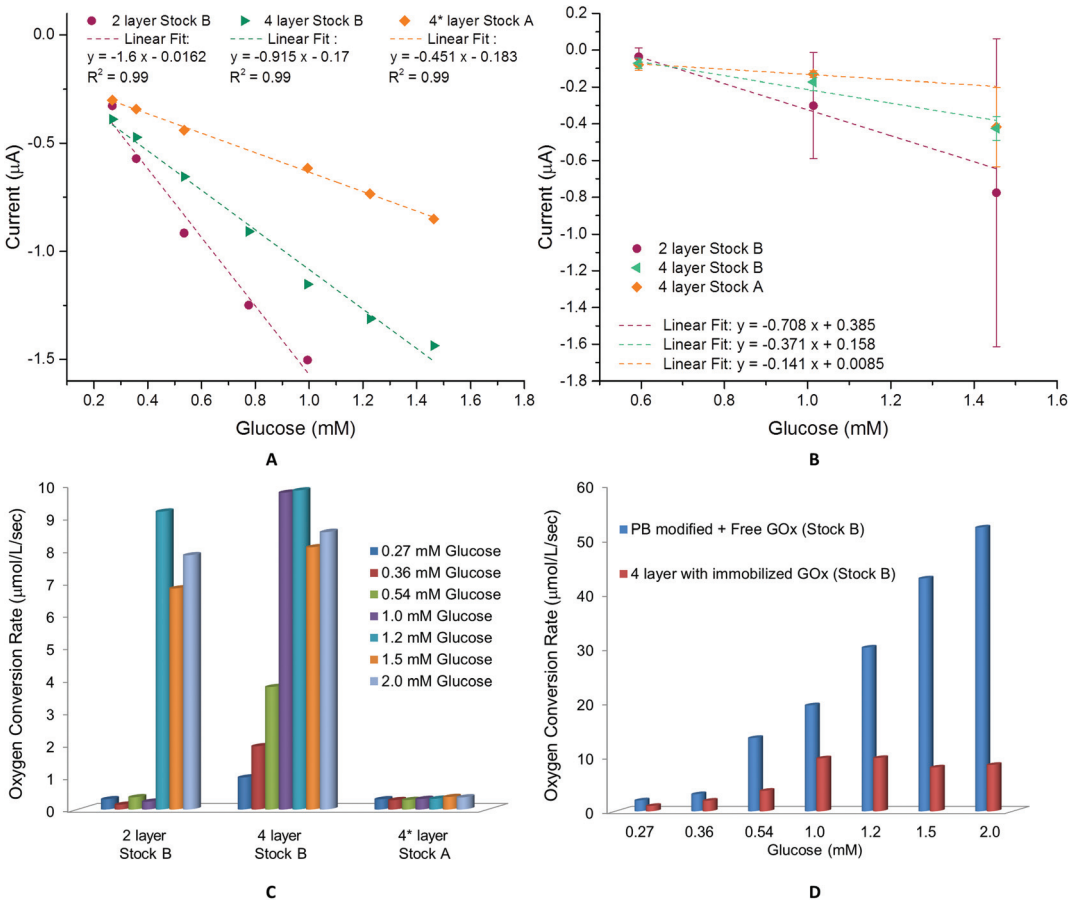

Fig. 2 The results of tandem monitoring of oxygen and glucose conversion rates during the characterization of "two" and "four" layer biosensors. The current response plotted towards the glucose concentrations in A corresponds to the first calibration for *2 layer Stock B* and *4 layer Stock B* and the second calibration (after 3 months) for *4*layer Stock A* glucose biosensors. In graph B the response obtained after the preparation of the same batches of *2 layer Stock B, 4 layer Stock B* and *4 layer Stock A* glucose biosensors is compared and plotted including standard deviations. The oxygen conversion rates obtained at different glucose concentrations (0.27–2 mM) for various glucose biosensors are shown in C and compared with PB modified ItalSens SPEs after the addition of glucose oxidase solution (Stock B) in D.

ESI†). Therefore, such a composition of "four" layer biosensors, namely the combination of the lower enzyme activity (Stock A) and the presence of an individual membrane layer (four layer architecture), prevents the strong perturbation of the glucose concentration in the droplet which is one of the requirements of the optimal biosensor performance.[17]

Comparing the behaviour of the GOx free in the solution over PB modified ItalSens SPEs and inside the "four" layer biosensors (Stock B) as shown in Fig. 2D, the expected reduction of catalytic activity is obtained after immobilization.[43–46] However, the oxygen deficit in the reaction of the free enzyme solution was already registered at 0.54 mM glucose concentration (see Table S2, ESI†) which again resulted in a limited detection range of PB modified SPEs (Fig. 3A). The residual activity of the free enzyme solutions registered during chronoamperometric characterization with glucose (see Table S2, ESI†) was approximately equal between PB modified DropSens (0.08 U μL^{-1} ± 0.09) and ItalSens (0.1 U μL^{-1} ± 0.1) SPEs. Although the difference in sensitivity for both types of PB modified SPEs is not so pronounced, the presence of graphene oxide (GO) significantly enhances the electrochemical response (see Table S2, ESI†) and improves the overall sensor performance. Thus, the extended linear detection range for the PB modified DropSens SPEs is attributed to the higher amount of the mediator deposited inside the cavities of GO[39] which was also obtained during cyclic voltammetry studies (Fig. 3B). Moreover, this explains the rapid oxygen conversion rates for the PB modified DropSens SPEs in comparison with ItalSens SPEs and confirms the significant role of the mediator concentration and electrode material in biosensor lifetime.

Therefore, the findings obtained within tandem monitoring are crucial because it allows getting closer insights into the principles of the glucose biosensor biorecognition mechanism, together with the simple visualization and quantification of the correlations between system parameters. Furthermore, the initial calibration curve and voltammograms obtained right after the preparation of "four layer" glucose biosensors (based on GOx Stock A solution) and then repeated after three months are presented in Fig. 3. The significant increase of the sensitivity and intercept values obtained

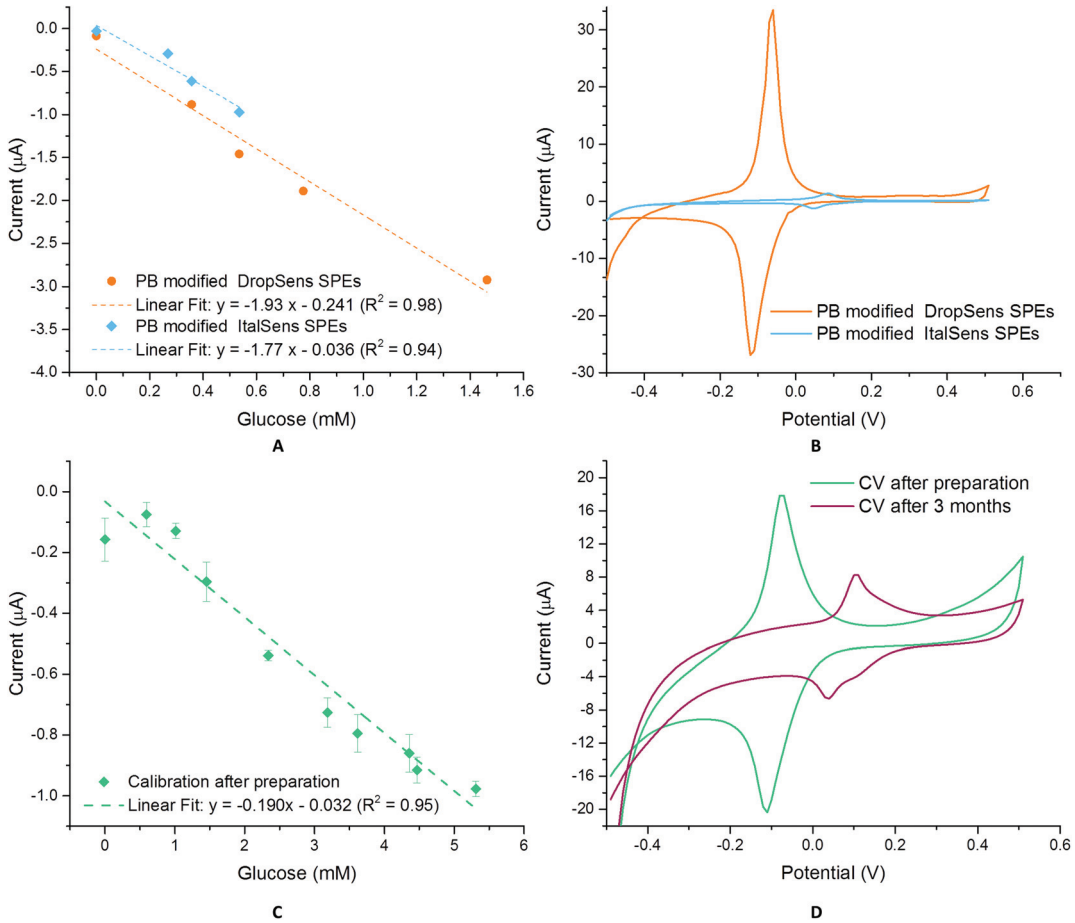

Fig. 3 Comparison of the amperometric calibration curves and cyclic voltammograms of PB modified SPEs and "four" layer glucose biosensors. The chronoamperometric response was registered for PB modified DropSens and ItalSens SPEs (A) in the presence of the free enzyme solution and plotted against the linear detection range of glucose concentrations (from 0.27 to 1.5 mM). The corresponding CVs registered in phosphate buffer at 20 mV s^{-1} scan rate prior to AM characterization are shown in B. The initial calibration curve and CVs obtained for a "four" layer glucose biosensor (Stock A) immediately after preparation and following three month storage are presented in C and D, respectively. The CVs were registered in phosphate buffer at 20 mV s^{-1} scan rate prior to AM characterization. The chronoamperometric response was plotted against the analytical range of glucose concentrations from 0.1 to 5.4 mM.

between the first (Fig. 3C) and second calibrations (Fig. 2A) can be attributed to the loss of the Prussian Blue from the GO layer registered during cyclic voltammetry studies (Fig. 3D). Since PB is involved in the reaction of hydrogen peroxide degradation, the composition of the probes collected after CV and AM measurements was analyzed with respect to iron elution (Fe^{56} isotope) in the following section.

3.2. The effect of operating conditions on the mediator elution and biosensor response

In the next step, the composition of the probes collected after AM and CV measurements was evaluated for the presence of Fe^{56} ions by means of inductively coupled plasma mass spectrometry (ICP-MS). The obtained results are summarized in Fig. 4. Comparing the behavior of glucose biosensors at the first CV scans registered at different scanning speeds (Fig. 4A), the Fe^{56} elution remains approximately constant for the "four" layer sensors regardless of the scan speed. On the other hand, summarizing the overall iron content obtained for the same period of time (approx. 202 s) the potential was varied at different scan rates (Fig. 4B), the PB layer showed a better stability for "two" layer glucose biosensors. The impact of the scan number on the mediator (PB) layer stability is presented for "two" and "four" layer biosensors in Fig. 4C and D, respectively. Interestingly, regardless of the biosensor design, with the increased number of scans a higher overall iron content was obtained in pure buffer samples. Such phenomena can be explained by the irreversible changes occurring from scan to scan in the local surface topography caused by both continuous iron elution from the insoluble mediator layer into the aqueous phase and the membrane film stability discussed in the following section 3.3. Therefore, the choice of right operating conditions would significantly affect the overall biosensor stability, response and lifetime. The optimal scan rate that minimizes the mediator leakage is 20 mV s^{-1} for both the "two" and the "four" layer biosensors.

The iron content of the AM probes collected after characterization with glucose of the "two" layer glucose biosensors

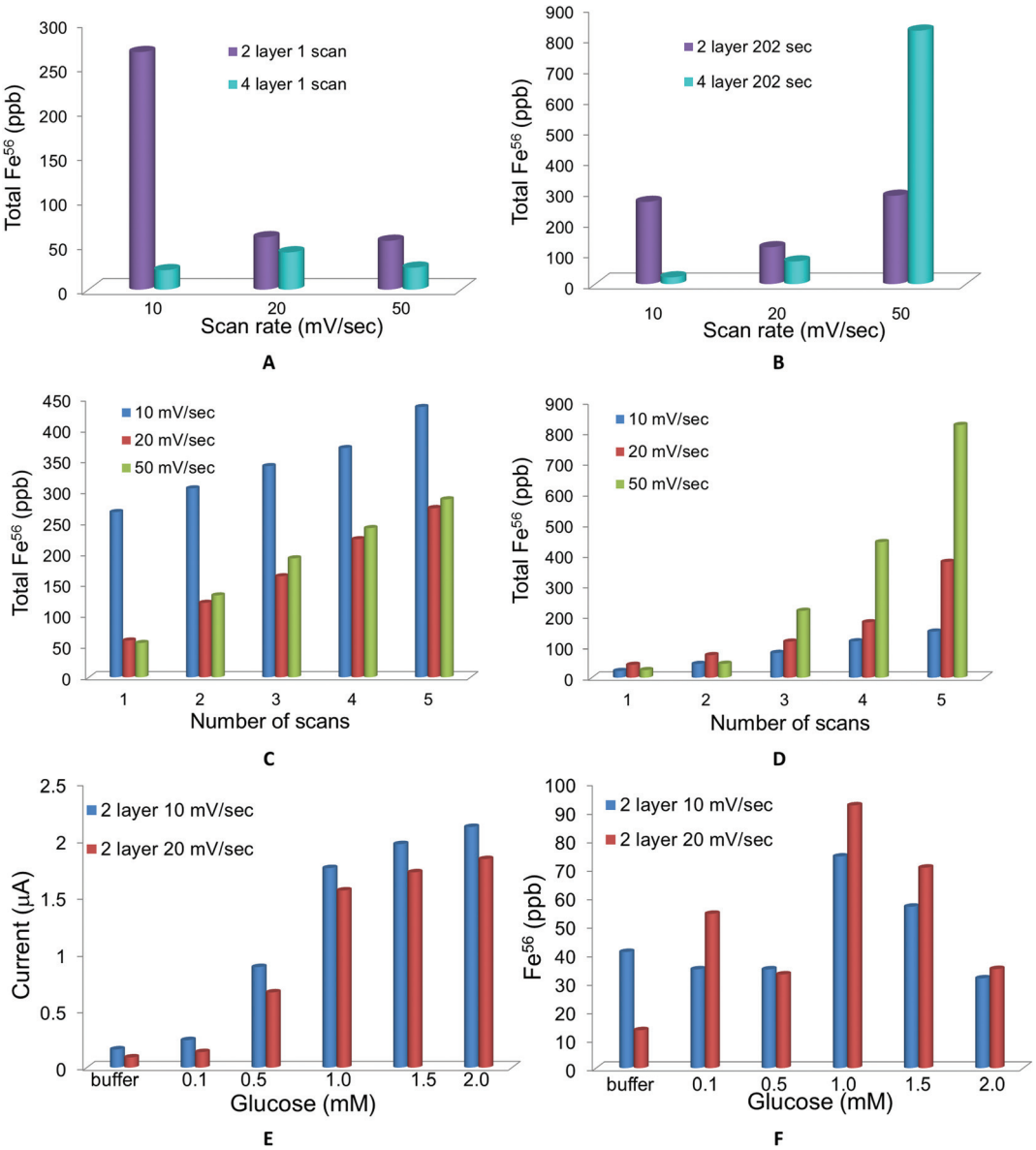

Fig. 4 Iron Fe^{56} elution during CV and AM studies for "two" and "four" layer glucose biosensors. The impact of the scan rate on the Fe^{56} leakage is summarized for the first scans (A) and for an equal amount of time (B) the potential was varied. The effect of the number of scans for various speeds is shown for "two" and "four" layer glucose biosensors in graphs C and D, respectively. For "two" layer glucose biosensors previously characterized at 10 and 20 mV s^{-1} scanning speed the results are shown for AM (E) and ICP-MS analysis (F). The RSD values for ICP-MS data is not shown due to the low values (less than 2%).

(Stock B) previously studied at different scan rates (10 and 20 mV s^{-1}) in cyclic voltammetry was identified using ICP-MS. In Fig. 4E it is shown that, similar to the results presented in Fig. 2, with a higher glucose concentration the absolute current value is increased and the sensor detection range is below 1 mM glucose concentration. Moreover, for both biosensors the equal voltammetric behaviour of Prussian Blue films measured prior to AM characterization resulted in quantitatively similar calibration curves (data are not shown). The increase of the iron content inside the probes at 1 mM concentration (Fig. 4F) could be related to a higher amount of peroxide produced during the oxidation of higher concentrations of glucose. However, the limited detection range and subsequent decrease in the iron elution rate for glucose solutions above a 1 mM concentration threshold indicates that the enzyme reaches the oxygen deficit phase. The overall iron loss for both biosensors during chronoamperometric characterization varied from 273 to 298 ppb.

3.3. The effect of operating and preparation conditions on membrane stability

The buffer probes collected after CV studies of "two" and "four" layer glucose biosensors were analyzed for their Nafion content using liquid chromatography electrospray ionization

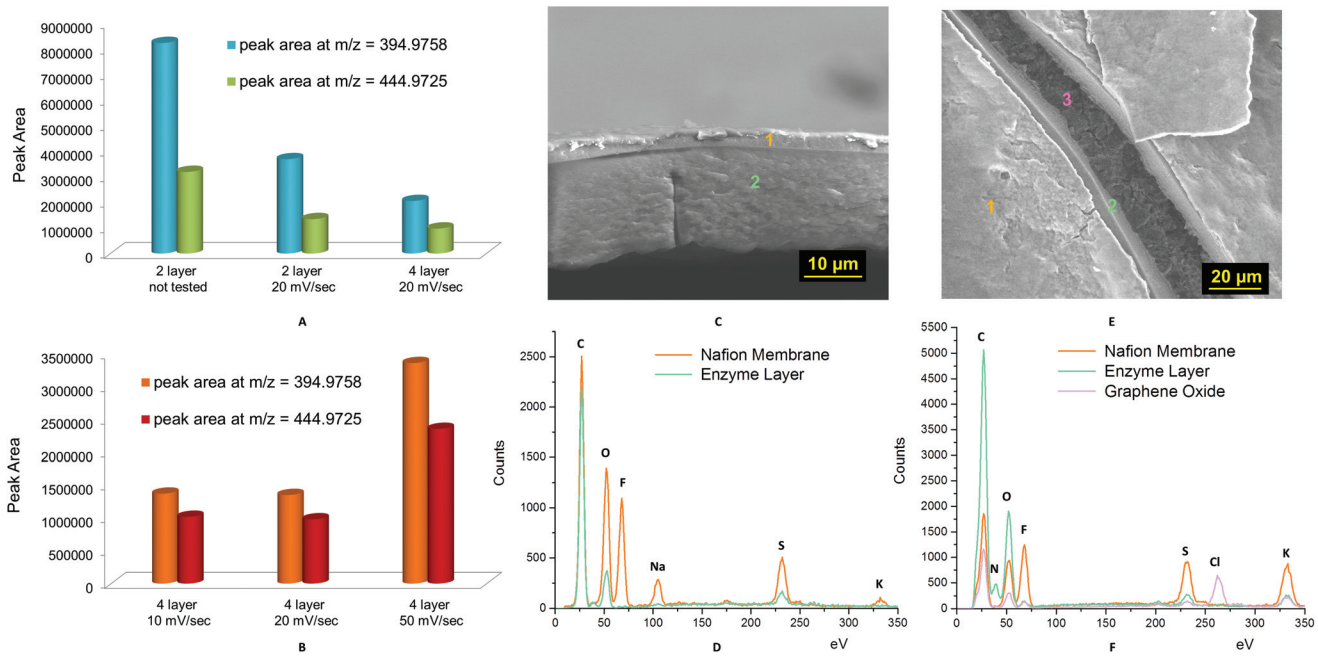

Fig. 5 The impact of the scan rate on the stability of the membrane layer. The mass spectra results were summarized for probes collected after first scans and correspond to peak areas of perfluorinated $CF_3(CF_2)_5CHFCOO^-$ and $CF_3(CF_2)_6CHFCOO^-$ carboxylic acid fragments registered at *m/z* 394.9758 and 444.9725, respectively. The influence of the equal scan rate (20 mV s^{-1}) on the "two" and "four" layer biosensors is shown in A. The effect of different scan rates on the "four" layer biosensors is presented in B. Note: the results were obtained from the same batch of biosensors measured in triplicate. RSD values (%) are too low to be shown. The individual enzyme (1) and membrane (2) layers of the "four" layer glucose biosensor are demonstrated by SEM images in cross-section (C) for a non-tested "four" layer glucose biosensor. The corresponding EDX spectrum is shown in D. The top view of the membrane (1), enzyme (2) and graphene oxide (3) layers is enlarged in E for the glucose biosensor characterized in CV and AM. The corresponding EDX spectrum is presented in F.

tandem mass spectrometry (LC-ESI-MS/MS). The dependence of the peak areas of the obtained characteristic Nafion-related fragments on the sensor design and the operation conditions is summarized in Fig. 5. From Fig. 5A it is evident that in comparison with the non-used biosensors tested in a steady state experiment with a water droplet, the glucose biosensors used in cyclic voltammetry studies possess a higher membrane stability especially in case of the "four" layer sensors. Moreover, no significant influence of the scan number on the membrane stabilization was observed for "four" layer biosensors (data not shown), contrary to the previously characterized "two" layer sensors.[39] Such phenomena can be partly explained by the influence of the applied potential (fixed or varied value, scanning speed, duration, *etc.*) on the final thickness of the polymeric films.[17] The more pronounced role of the scanning speed on the Nafion elution rates was demonstrated in Fig. 5B. Regardless the biosensor composition, the lower scanning speed, namely 20 mV s^{-1}, allows for the faster stabilization of the membrane layer during cyclic voltammetry studies. The architecture of the "four" layer glucose biosensors was confirmed by the subsequent SEM/EDX studies. From the obtained results, it is clear that the double deposition of 2% Nafion coatings over the enzymatic layer yields a formation of a uniform membrane film (Fig. 5C and D). Moreover, the Nafion layer remains fixed on top of the glucose oxidase surface after performing cyclic voltammetry and chronoamperometric measurements (Fig. 5E and F). Numerous membrane cracks registered under vacuum in SEM on the surface of both tested and not tested "two" and "four" layer glucose biosensors were further investigated using environmental scanning electron microscopy (ESEM).

3.4. The impact of environmental conditions on membrane film formation

The membrane swelling of the wetted glucose biosensors was confirmed under dynamic conditions at different temperatures by varying the water vapor pressure inside the ESEM chamber (see Fig. S6, ESI†). The formation of water droplets on top of the biosensor layers is visible (see Fig. S6C, D, G and H, ESI†). Thus, the ESEM analysis demonstrated that the cracks observed in the enzyme and/or membrane films would transform to the monolayer being in contact with water-based analyte solutions. In the next step, the role of the environmental conditions, *viz.* temperature and humidity, upon membrane layer formation was evaluated experimentally. For this purpose, we have analyzed the biosensors after the enzyme/membrane layer was dried at 20 °C (approx. 70% humidity) and 8 °C (40% humidity maintained in the climate chamber) for 15 min and 12 hours, respectively. The results obtained *via* multi-analytical studies are summarized in Fig. 6 (shown for "two" layer glucose biosensors).

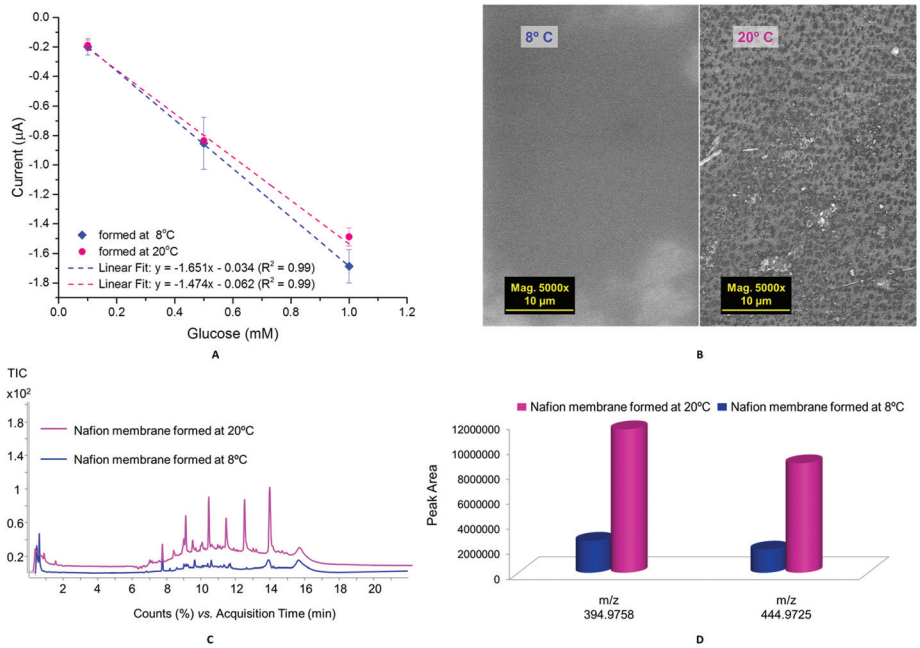

Fig. 6 The results of the multi-analytical analysis of "two" layer glucose biosensors (enzyme/membrane layer formed at 8 °C or 20 °C). The linear current response towards glucose is presented in A. SEM images of the enzyme/membrane (top view) were enlarged in B. The total ion chromatograms (TICs) registered for the Nafion content in buffer probes collected after CV measurements performed at 10 mV sec^{-1} are plotted in C. The EIC mass spectra results shown in D correspond with peak areas of perfluorinated $CF_3(CF_2)_5CHFCOO^-$ and $CF_3(CF_2)_6CHFCOO^-$ carboxylic acid fragments registered at *m/z* 394.9758 and 444.9725, respectively.

Although no significant difference in the sensitivity and detection range between the two designs of biosensors was observed after the first calibration (Fig. 6A), the subsequent chronoamperometric studies with glucose resulted in a strong variation of the biosensor response when the polymeric film was formed at 20 °C (*e.g.* the obtained results did not fit the calibration curve). The obtained phenomena can be partly attributed to the numerous membrane defects formed at 20 °C that were revealed during SEM investigations (Fig. 6B). The dependency of the membrane layer formation on the environmental conditions was fully confirmed by further analysis of the collected buffer probes by means of LC-ESI-MS/MS (Fig. 6C and D). Thus, the mild drying conditions, namely 8 °C and 40% humidity maintained in a climate chamber, allow for a uniform layer formation which is better fixed on the surface of the biosensor (the polymer leakage decreased almost 6 times).

4. Conclusions and future perspectives

The analytical approach for simultaneous multiple-substrate monitoring for biosensors in a droplet was proposed. The presented methodology was validated for first generation glucose biosensors with a different layer-by-layer assembly in the presence of glucose. The results obtained *via* combined chronoamperometric characterization and oxygen monitoring were independently confirmed by the subsequent morphological and chemical studies. The conclusions for different sections of the work performed can be summarized in the following points:

- The specific protocols developed for the detection of oxygen conversion, iron and Nafion elution rates inside the biosensor system allowed identifying a more favorable structure, and suitable operating conditions for the biosensors.
- It was shown that the variation of the immobilized enzyme activity, electrode material, additional membrane films and experimental conditions for the layer formation can significantly improve the lifetime and the detection range of the biosensors.
- It was proven that the choice of the right CV conditions would predetermine the future chronoamperometric behaviour of the biosensor. Moreover, the stability of the mediator and membrane layers plays an important role in the changes in the biosensor response (*i.e.* sensitivity, detection range, *etc.*) during second calibration and eventually prevents inactivation of the enzyme.
- The presence of individual Nafion coatings in "four" layer glucose biosensors allowed to enhance the overall biosensor stability (up to 3 months) and to extend the linear detection range by up to a factor of five even with an enzymatic layer having a lower activity in comparison with the "two" layer glucose biosensors.
- The presented analytical assay allows tracking the impact of biosensor parameters and architecture changes on its overall analytical performance, the mass transfer processes and the biorecognition mechanisms. Moreover, the demon-

strated tandem monitoring approach allows minimizing the chemical usage and waste generation.

The practical merit of the presented work is in the development of a universal time- and cost-effective methodology that can be applied for screening of the optimal design of amperometric biosensors based on the oxygen dependent processes. The presented tandem monitoring approach can significantly improve the quality control of the biosensors at the development stage and facilitate the overall concept-to-market evaluation process. Moreover, it can be also used in studying purposes for a better understanding of the mechanisms behind the sensor's response. As future work, the tandem monitoring approach will be further evaluated in the presence of fermentation samples and implemented for screening biosensors based on other oxidases (for *e.g.* alcohol or lactate oxidase).

Conflicts of interest

The authors declare no conflict of interest.

Acknowledgements

This research was supported by the EUROMBR project that received funding from the People Programme (Marie Curie Actions, Multi-ITN) of the European Union's Seventh Framework Programme for research, technological development and demonstration (grant agreement no. 608104). The authors would like to acknowledge Mafalda Dias Gomes (PROSYS, DTU), Claudia Fink-Straube (Chemical Analytics, INM) and Anne Ladegaard Skov (DPC, DTU) for their support and for providing access to their instrumentation.

References

1 J. Wang, *Sens. Update*, 2002, **10**, 107–119.
2 A. Heller and B. Feldman, *Chem. Rev.*, 2008, **108**, 2482–2505.
3 J. Wang, *Electrochem. Sensors, Biosens. Biomed. Appl.*, 2008, 57–69.
4 C. Chen, Q. Xie, D. Yang, H. Xiao, Y. Fu, Y. Tan and S. Yao, *RSC Adv.*, 2013, **3**, 4473–4491.
5 D. Bruen, C. Delaney, L. Florea and D. Diamond, *Sensors*, 2017, **17**, 1–21.
6 A. Salek-Maghsoudi, F. Vakhshiteh, R. Torabi, S. Hassani, M. R. Ganjali, P. Norouzi, M. Hosseini and M. Abdollahi, *Biosens. Bioelectron.*, 2018, **99**, 122–135.
7 O. Schnell, K. Barnard, R. Bergenstal, E. Bosi, B. Guerci, T. Haak, I. B. Hirsch and F. Snoek, *Diabetes Technol. Ther.*, 2017, **19**, 391–399.
8 J. R. Petrie, A. L. Peters, R. M. Bergenstal, R. W. Holl, G. A. Fleming and L. Heinemann, *Diabetes Care*, 2017, **40**, 1614–1621.
9 M.-N. Pons, *Curr. Opin. Biotechnol.*, 1993, **4**, 183–187.
10 J. Shi, D. Feng and Y. Li, in *Fermentation Processes*, ed. A. F. Jozala, InTech, 2017, vol. 6, p. 310.
11 M. Pohlscheidt, S. Charaniya, C. Bork, M. Jenzsch, T. L. Noetzel and A. Luebbrert, in *Upstream Industrial Biotechnology: Equipment, Process Design, Sensing, Control, and cGMP Operations*, ed. M. C. Flickinger, © 2013 JohnWiley & Sons, Inc., 1st edn, 2013, pp. 1469–1492.
12 M. Mehrvar and M. Abdi, *Anal. Sci.*, 2004, **8**, 14.
13 D. Grieshaber, R. Mackenzie, J. Vörös and E. Reimhult, *Sensors*, 2008, **8**, 1400–1458.
14 H. A. Abdulbari and E. A. M. Basheer, *ChemBioEng Rev.*, 2017, **4**, 92–105.
15 R. Săndulescu, M. Tertiș, C. Cristea and E. Bodoki, in *Biosensors - Micro and Nanoscale Applications*, 2015, p. 456.
16 D. Semenova, K. V. Gernaey and Y. E. Silina, *Analyst*, 2018, **143**, 5646–5669.
17 M. D. Ward and W. Kenneth, *J. Diabetes Sci. Technol.*, 2007, **1**, 201–204.
18 M. Arya and R. Arya, in *Advances in Biotechnology*, ed. I. Ravi, M. Baunthiyal and J. Saxena, 2014, p. 260.
19 N. Bhalla, P. Jolly, N. Formisano and P. Estrela, *Essays Biochem.*, 2016, **60**, 1–8.
20 A. Ambrózy, L. Hlavatá and J. Labuda, *Acta Chim. Slovaca*, 2013, **6**, 35–41.
21 C. Heitner-Wirguin, *Recent Adv. Perfluorinated Membr. Struct. Prop. Appl.*, 1996, **120**, 1–33.
22 S. Banerjee and D. E. Curtin, *J. Fluorine Chem.*, 2004, **125**, 1211–1216.
23 Y. Lv, F. Wang, H. Zhu, X. Zou, C. Tao and J. Wang, *Nanomater. Nanotechnol.*, 2016, **6**, 2–8.
24 A. A. Karyakin, E. A. Kotel'nikova, L. V. Lukachova and E. E. Karyakina, *Anal. Chem.*, 2002, **74**, 1597–1603.
25 F. Ricci, A. Amine, C. S. Tuta, A. A. Ciucu, F. Lucarelli, G. Palleschi and D. Moscone, *Anal. Chim. Acta*, 2003, **485**, 111–120.
26 U. Latif, F. L. Dickert, R. Blach and H. Feucht, *J. Chem. Soc. Pak.*, 2013, **35**, 17–22.
27 R. Tipnis, S. Vaddiraju, F. Jain, D. J. Burgess and F. Papadimitrakopoulos, *J. Diabetes Sci. Technol.*, 2007, **1**, 193–200.
28 T. Matsumoto, A. Ohashi, N. Ito, H. Fujiwara and T. Matsumoto, *Biosens. Bioelectron.*, 2001, **16**, 271–276.
29 J. Lu, L. T. Drzal, R. M. Worden and I. Lee, *Chem. Mater.*, 2007, **19**, 6240–6246.
30 A. Kusoglu and A. Z. Weber, *Chem. Rev.*, 2017, **117**, 987–1104.
31 L. Chaabane, L. Dammak, D. Grande, C. Larchet, P. Huguet, S. V. Nikonenko and V. V. Nikonenko, *J. Membr. Sci.*, 2011, **377**, 54–64.
32 J. A. Elliott, S. Hanna, A. M. S. Elliott and G. E. Cooley, *Polymer*, 2001, **42**, 2251–2253.
33 Y. Freijanes, V. M. Barragán and S. Muñoz, *J. Membr. Sci.*, 2016, **510**, 79–90.
34 M. A. Modestino, A. Kusoglu, A. Hexemer, A. Z. Weber and R. A. Segalman, *Macromolecules*, 2012, **45**, 4681–4688.
35 P. Vanya, J. Sharman and J. A. Elliott, *J. Chem. Phys.*, 2017, **147**, 1–9.

36 L. Fang, B. Liang, G. Yang, Y. Hu, Q. Zhu and X. Ye, *Biosens. Bioelectron.*, 2014, **56**, 91–96.
37 F. Ivanauskas, P. Katauskis and V. Laurinavičius, *J. Math. Chem.*, 2013, **52**, 689–702.
38 I. Grabowska, M. Sajnoga, M. Juchniewicz, M. Chudy, A. Dybko and Z. Brzozka, *Microelectron. Eng.*, 2007, **84**, 1741–1743.
39 D. Semenova, A. Zubov, Y. E. Silina, L. Micheli, M. Koch, A. C. Fernandes and K. V. Gernaey, *Sens. Actuators, B*, 2018, **259**, 945–955.
40 M. Mahosenaho, F. Caprio, L. Micheli, A. M. Sesay, G. Palleschi and V. Virtanen, *Microchim. Acta*, 2010, **170**, 243–249.
41 A. Nováková, L. Schreiberová and I. Schreiber, *Russ. J. Phys. Chem. A*, 2011, **85**, 2305–2309.
42 D. A. Ellis, S. A. Mabury, J. W. Martin and D. C. G. Muir, *Nature*, 2001, **412**, 321–324.
43 A. A. Homaei, R. Sariri, F. Vianello and R. Stevanato, *J. Chem. Biol.*, 2013, **6**, 185–205.
44 J. M. Harris, C. Reyes and G. P. Lopez, *J. Diabetes Sci. Technol.*, 2013, **7**, 1030–1038.
45 G. Rocchitta, A. Spanu, S. Babudieri, G. Latte, G. Madeddu, G. Galleri, S. Nuvoli, P. Bagella, M. I. Demartis, V. Fiore, R. Manetti and P. A. Serra, *Sensors*, 2016, **16**, 1–21.
46 S. Liébana and G. A. Drago, *Essays Biochem.*, 2016, **60**, 59–68.

